Geophysical Journal International

Geophys. J. Int. (2013) doi: 10.1093/gji/ggt385

Geophysical Journal International Advance Access published November 20, 2013

Quantifying potential earthquake and tsunami hazard in the Lesser Antilles subduction zone of the Caribbean region

Gavin P. Hayes,[1] Daniel E. McNamara,[1] Lily Seidman[1,*] and Jean Roger[2]

[1] *U.S. Geological Survey National Earthquake Information Center,* 1711 *Illinois St, Golden, CO* 80401*, USA. E-mail: ghayes@usgs.gov*
[2] *UFR Sciences Exactes et Naturelles, Université Antilles Guyane, Fouillole - BP* 250 – 97157*, Pointe-à-Pitre, France*

Accepted 2013 September 20. Received 2013 September 17; in original form 2013 June 20

SUMMARY

In this study, we quantify the seismic and tsunami hazard in the Lesser Antilles subduction zone, focusing on the plate interface offshore of Guadeloupe. We compare potential strain accumulated via GPS-derived plate motions to strain release due to earthquakes that have occurred over the past 110 yr, and compute the resulting moment deficit. Our results suggest that enough strain is currently stored in the seismogenic zone of the Lesser Antilles subduction arc in the region of Guadeloupe to cause a large and damaging earthquake of magnitude $M_w \sim 8.2 \pm 0.4$. We model several scenario earthquakes over this magnitude range, using a variety of earthquake magnitudes and rupture areas, and utilizing the USGS ShakeMap and PAGER software packages. Strong ground shaking during the earthquake will likely cause loss of life and damage estimated to be in the range of several tens to several hundreds of fatalities and hundreds of millions to potentially billions of U.S. dollars of damage. In addition, such an event could produce a significant tsunami. Modelled tsunamis resulting from these scenario earthquakes predict meter-scale wave amplitudes even for events at the lower end of our magnitude range (*M* 7.8), and heights of over 3 m in several locations with our favoured scenario (*M* 8.0, partially locked interface from 15–45 km depth). In all scenarios, only short lead-times (on the order of tens of minutes) would be possible in the Caribbean before the arrival of damaging waves.

Key words: Tsunamis; Earthquake ground motions; Seismicity and tectonics; Subduction zone processes; Atlantic Ocean.

INTRODUCTION

Although earthquake and tsunami hazards in the Caribbean have been the focus of many studies over the past 30 yr, relatively few have analysed in detail the hazards associated with the Lesser Antilles arc (e.g. Stein *et al*. 1982; McCann & Sykes 1984; Bernard & Lambert 1988; Shepherd 1992; Feuillet *et al*. 2002, 2011; Roger *et al*. 2013), focusing instead on the perhaps greater and more proximate dangers, relative to the eastern seaboard of the United States and the highly populated islands of the northern Caribbean (e.g. Calais *et al*. 1998; Dolan & Wald 1998; Mann *et al*. 2002, 2005; Prentice *et al*. 2003; ten Brink & Lin 2004; ten Brink *et al*. 2009, 2011; Geist & Parsons 2009; Geist *et al*. 2009). However, though the majority of the large damaging earthquakes in the Caribbean have occurred within the northern plate boundary zone, the relatively less complex subduction zone of the Lesser Antilles arc farther south has also hosted such earthquakes in the past, most notably in 1843 when a *M*7.5–8.5 earthquake killed several thousand people on Guadeloupe and surrounding islands (Robson 1964). Were such an event to occur in the same region today, the effects would potentially be more catastrophic to an increasingly vulnerable region that has seen significant population densification in the past 40–50 yr (Hyman 2005) and currently hosts an estimated 500 000 daily beach visitors, a majority of whom are not likely aware of tsunamigenic earthquake hazards (Proenza & Maul 2010).

Several of these past studies (e.g. McCann & Sykes 1984; Bernard & Lambert 1988) attempted to quantify potential seismic hazard in the Lesser Antilles subduction zone based on the size of large historic earthquakes, as discussed in the next section. More recently, Geist *et al*. (2009) used the historic earthquake record of the whole Caribbean (CA): North America (NA): South America (SA) Plate boundary system to estimate the margins' maximum credible earthquake magnitude and recurrence times empirically for tsunami hazard probability. Maximum magnitude was calculated using a slip rate given by tectonic loading (plate motions), by assuming the seismogenic zone of the plate boundary is 100 per cent coupled, and that the whole length of the margin (∼1100 km, the length of the

*Now at: Department of Earth Science, Rice University, MS-126, 6100 Main Street, Houston, TX 77005, USA.

subduction margin from Hispaniola to an approximate location for the CA:NA:SA triple junction) could rupture in one event, with a magnitude range M_{max} ~ 8.95–9.58. Although such an event has not been witnessed in ~500 yr of recorded history in the region, and the likelihood of rupturing the entire seismogenic zone in one event is low given the pattern of historic events, the return time predicted from these empirical relationships for an earthquake of $M > 8.5$ is ~1000 yr. As this earthquake cycle is longer than the span of our records, the occurrence of such an event cannot be ruled out. It is also prudent to note that the two most recent catastrophic tsunamigenic earthquakes globally occurred on subduction zone segments where events of their size were unanticipated (i.e. Sumatra in 2004 and Tohoku in 2011).

We attempt to build on these past studies using a compilation of seismicity catalogues over the past ~110 yr to quantify the earthquake potential for the Lesser Antilles subduction zone based on strain accumulation from plate motions, and patterns of strain release during earthquakes. Whereas earthquake catalogues for the Caribbean region extend as far back as 1500 (e.g. Shepherd & Lynch 1992; Lynch & Shepherd 1995), older records are not detailed enough to permit accurate locations, nor to categorically discriminate between subduction and non-subduction events. For these reasons, we choose to focus on the more recent history with better-known earthquake locations. Such a comparison allows us to establish where significant moment deficit exists today—where strain has accumulated as a result of continued plate motions, but has not been released seismically—providing a quantified estimate of the current seismic potential of the region.

TECTONIC SETTING

Along the northern and central portion of the Lesser Antilles arc (between ~14°N and 19°N) relative motion between the NA and CA plates is taken up by convergence and subduction of Atlantic oceanic seafloor beneath the arc at a rate of ~2 cm yr^{-1}, in an WSW direction (DeMets *et al*. 2000, 2010; Fig. 1). Farther north, motion between the two plates is taken up by oblique convergence at the Puerto Rico trench and left-lateral strike-slip motion along several major transform systems in a broad plate boundary zone surrounding Puerto Rico and Hispaniola (Mann *et al*. 1995; Feuillet *et al*. 2002). In the southern portion of the arc, relative motion is presumably occurring between the South American and Caribbean plates, but because the boundary between the North and South American plates is rather diffuse and accommodates a very low rate of relative motion, convergence rate and direction in the southern Lesser Antilles is approximately the same as that in the north, subducting Atlantic seafloor in a WSW direction (e.g. Jordan 1975; Stein *et al*. 1982). Farther south still, near Trinidad and Tobago and to the north of Venezuela, motion between the Caribbean and South American plates is taken up by dextral strike-slip motion along the El-Pilar Central Range fault zone (Weber *et al*. 2001; Feuillet *et al*. 2002).

Where subduction of Atlantic oceanic crust is occurring in a direction nearly perpendicular to the trench (roughly between ~12°N and 19°N), the Lesser Antilles arc has formed 200–400 km to the west, behind a thick accretionary prism. This arc comprises a western strand of volcanic islands, and an eastern non-volcanic strand

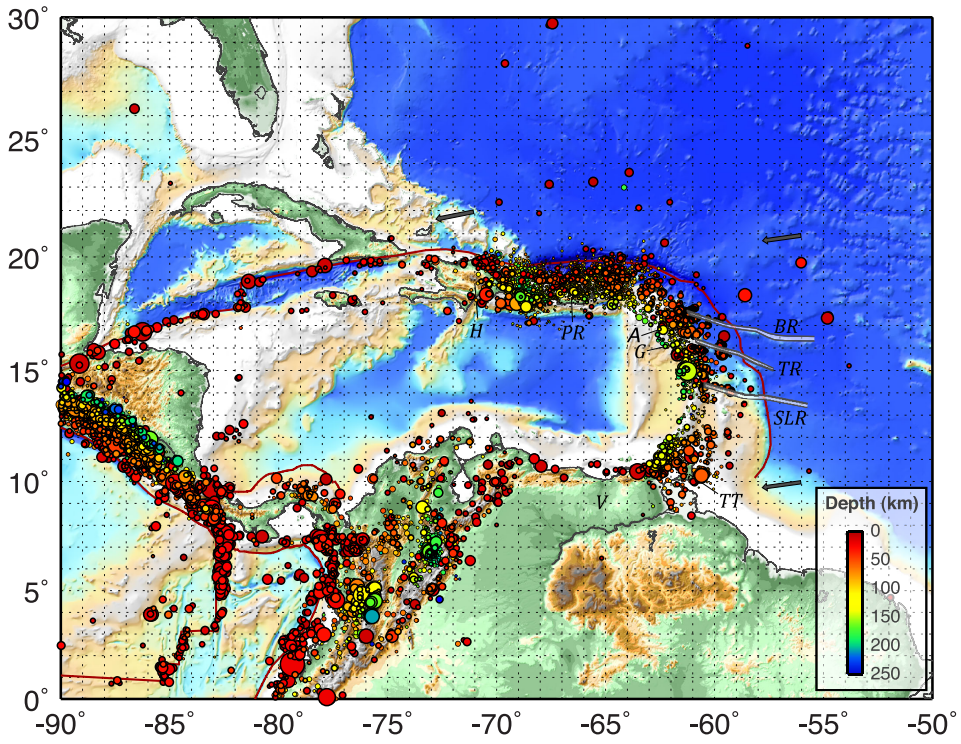

Figure 1. Map of the tectonic setting of the Lesser Antilles Arc and the broader Caribbean region. The Lesser Antilles subduction zone is the north–south portion of the broader Caribbean Arc, from ~10°N to 19°N, where plate convergence is approximately perpendicular. Circles with bold black outlines show earthquakes from the EHB catalogue, sized by magnitude and coloured by depth. Circles with light outlines are earthquakes from the USGS PDE. Grey arrows represent North America–Caribbean Plate motions from DeMets *et al*. (2000). Maroon lines demarcate major plate boundaries; white shaded polygons with grey outlines represent the approximate locations of the Barracuda (BR), Tiburon (TR) and Saint Lucia (LCR) Ridges. Islands and countries discussed in the main text are labeled: Hispaniola (H), Puerto Rico (PR), Antigua (A), Guadeloupe (G), Trinidad and Tobago (TT) and Venezuela (V).

of coral limestone, the separation of which may be related to the kinematic history of the plate boundary (Bouysse & Westercamp 1990; Feuillet *et al*. 2002). In several places along the subduction zone, particularly in the region adjacent to and south of Guadeloupe, bathymetric highs intersect the trench. Of particular interest here are the Barracuda, Tiburon and Saint Lucia Ridges, which may affect seismogenic properties of the subduction thrust farther downdip (e.g. Stein *et al*. 1982; McCann & Sykes 1984; Bernard & Lambert 1988). A more recent study (Laigle *et al*. 2013) confirms that these ridge structures may cause along-arc segmentation, though as those authors point out, such segmentation may not prevent the propagation of extremely large ruptures like the *M* 9.0 2011 March Tohoku earthquake.

HISTORIC SEISMICITY AND PAST STUDIES

Several authors have attempted to quantify past seismicity and seismic hazard in the Lesser Antilles Arc (Stein *et al*. 1982; McCann & Sykes 1984; Bernard & Lambert 1988). Stein *et al*. (1982) studied mechanisms of earthquakes along the subduction zone between 1950 and 1978, and showed a general lack of subduction-thrust activity, concluding that either the subduction zone here is decoupled, or that the time period studied was unrepresentative of the earthquake cycle of the subduction zone.

McCann & Sykes (1984) examined the role of subducting aseismic ridges in the tectonics and seismic potential of the region, suggesting that the Barracuda Ridge in the north, and the Tiburon and Saint Lucia Ridges in the south (Fig. 1) may create segmentation of the arc and act as barriers to rupture propagation during a subduction thrust earthquake. They showed that these ridges may have played a role in arresting the ruptures of the largest known historic earthquakes in the northcentral arc region: the 1843 event offshore of Guadeloupe which they estimated as $M8.25 \pm 0.25$, rupturing a segment of the subduction thrust ∼275 km long, and a smaller earthquake offshore of Saint Lucia in 1839 of *M*7.0–7.5. Farther south (south of ∼14°N), these authors highlighted the lack of shallow thrust events in the past 400 yr, though a deeper (∼60 km) ∼*M*7.4 earthquake caused damage in Venezuela in 1888.

Bernard & Lambert (1988) revisited many of the felt report references for the 1843 earthquake to revise estimates of the size of this event, suggesting the earthquake was more likely *M*7.5–8.0 with a rupture zone extending only ∼100 km, compatible with rupture on the subduction thrust bounded in the north and south, respectively, by the Barracuda and Tiburon Ridges. Although these authors discuss seismic hazard for the region, their results are mainly focused on shallow intraplate normal-faulting events that have been damaging in the past and are capable of generating significant tsunamis. They discuss the potential for large interplate thrust earthquakes similar to the 1843 event and also highlight the role of the subducting aseismic ridges in the region as potential barriers for rupture propagation.

The 1843 earthquake was analysed further in separate studies by Feuillet *et al*. (2011) and Hough (2013), and briefly by ten Brink *et al*. (2011). The latter study determined an intensity-based magnitude of *M* 7.8 with a 2σ range of *M* 7.6–8.4. Feuillet *et al*. (2011) use intensities reported in Robson (1964), Bernard & Lambert (1988) and Shepherd (1992), to assign a magnitude of *M* 8.5, and an approximate rupture length of 300 km; Hough (2013) used these felt intensities and additional reports from the United States to estimate M_w 8.4, with values as high as M_w 8.5–8.7 if the earthquake occurred farther offshore than its generally preferred location beneath the islands of Guadeloupe. Feuillet *et al*. (2011) noted that the lack of significant tsunami observations is likely indicative of rupture of the deeper portion of the megathrust plate interface in the region.

A recent study by Parsons & Geist (2008) specifically assessed tsunami run-up probability in the region by running empirical simulations based on the historic tsunami catalogue of O'Laughlin & Lander (2003), and by comparing them to numerical simulations based on finite-element, moment-balance models of the NA:CA plate boundary. Although they show that seismicity rates can be satisfied by a plate boundary coupling coefficient of 0.32, they note that both tsunami and seismicity catalogues may be incomplete and thus not representative of the true hazard in the region; a parameter they then pursue probabilistically via scenario models. Here, instead, we assume that the catalogue is incomplete (based on the recognition of large events in the past that have not recurred more recently), and use moment deficit calculations to quantify the potential size of future events.

Tsunamis associated with large earthquakes in the Lesser Antilles region are also a hazard that must be considered and quantified. Since the devastating Haiti earthquake of 2010 January, awareness of population and infrastructure vulnerability from earthquake shaking has increased in the Caribbean region. However, a significant tsunami event has not occurred in ocean basins of the Atlantic and Caribbean within the lifetime of most residents and structures. For this reason there is still a general lack of awareness and understanding of the destruction that such an event could cause. Historical data suggest that the Caribbean Basin and particularly the Lesser Antilles islands have been impacted by several tsunamis over the past 500 yr (O'Loughlin & Lander 2003). In addition to local earthquakes, the Caribbean region is at risk from a tsunami generated by other mechanisms such as distant earthquakes, undersea landslides and volcanic activity. Devastating tsunamis that affected the region include the 1755 Lisbon transoceanic tsunami (Roger *et al*. 2010a,b; Zahibo *et al*. 2011) and the regional 1690 Nevis and St Thomas (O'Loughlin & Lander 2003) and 1867 Virgin Islands (Zahibo *et al*. 2003) tsunamis.

Several locally generated tsunamis are known to have impacted the islands of the Lesser Antilles, and specifically Guadeloupe. The most significant of these was due to pyroclastic flows from the La Soufrière Hills volcano on Montserrat in 2003 July. The flows spilled into the sea generating a 1- to 2-m high tsunami that struck northeastern Guadeloupe (Pelinovsky *et al*. 2004). In addition, the 2004 Le Saintes (M_w 6.3) earthquake occurred in the Dominica Passage that separates Guadeloupe from Dominica. Strong shaking, with intensities as high as MMI VII were reported and the earthquake was large and shallow (14 km) enough to generate a weak tsunami with maximum run-up amplitudes of 70–80 cm on neighbouring islands (Le Friant *et al*. 2008).

These studies thus lay the context for large subduction thrust earthquakes and damaging tsunamis in the past, and highlight the lack of significant large earthquakes since the nineteenth century, indicative of the potential for large events and tsunamis in this region in the future. We attempt to update these studies, specifically to quantify how big such an event might be based on comparisons between strain accumulation and release in the subduction zone over the past 100+ yr. We then analyse the shaking and tsunami impact of scenario earthquakes local to Guadeloupe to quantify the risk of such events to local populations.

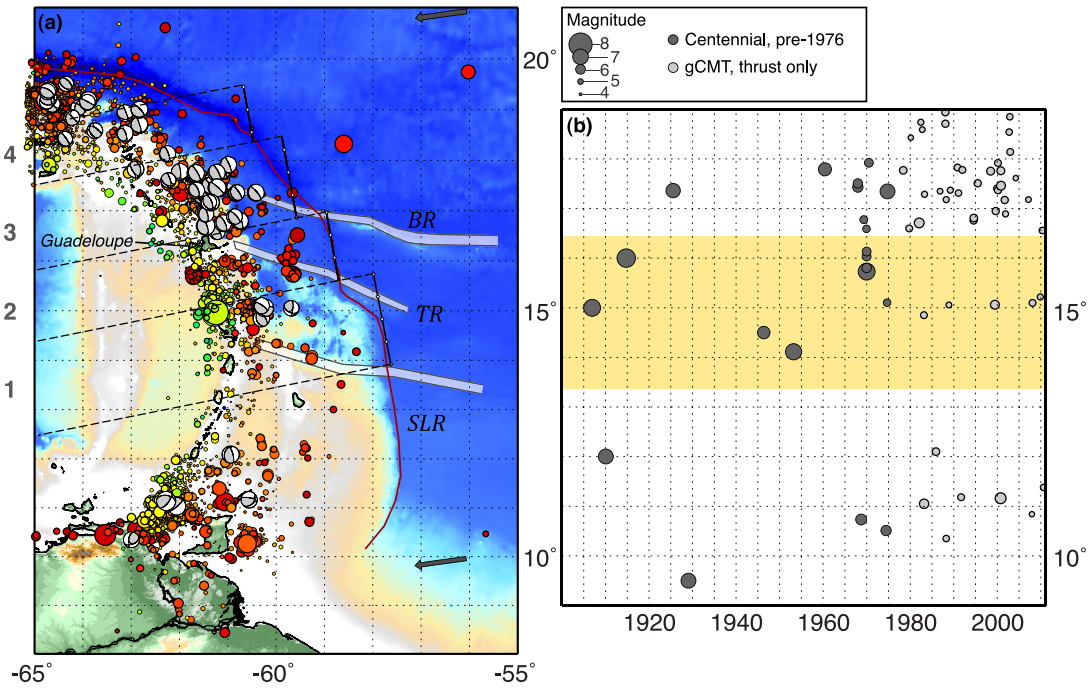

Figure 2. (a) Zoomed map of the study area. Grey focal mechanisms are thrust earthquakes from the gCMT catalogue, plotted at their respective EHB locations. Black dashed lines delimit 4 cross-sectional areas used for moment deficit calculations (1–4; see Fig. 3). See Fig. 1 caption for other symbology. (b) Plot of earthquake latitude with time since 1900. Light grey circles represent gCMT thrust earthquakes plotted in (a); dark grey are all earthquakes in study region from the Centennial Catalogue prior to 1976 (the start of the gCMT catalogue). Shaded yellow region represents the approximate area of our moment deficit calculation.

REGIONAL SEISMICITY

The Lesser Antilles Subduction zone has hosted very few moderate-large sized earthquakes in recent history. Since 1900, just 26 earthquakes of $M > 6$ have been recorded teleseismically, 6 of which were $M > 7$, most recently off the coast of Martinique in 2007 November (M 7.4, $Z \sim 150$ km, USGS). None of these events were as large as $M8$ and only one of the 16 $M > 6$ events since 1973 was a thrust-faulting event likely associated with slip on the subduction thrust interface; in total, since 1973, just 30 thrust-faulting events of $M > 5$ in this subduction zone have been recorded teleseismically, mainly restricted to the northern end of the arc offshore of Antigua (Fig. 1). The subduction zone offshore of Guadeloupe, and for an extent ~300 km to the south, is clearly defined by small ($M < 5$) earthquakes, but has only hosted two moderate-large events within its' seismogenic zone in the past ~40 yr, and just a few more since 1900 (Fig. 2).

These low rates of seismicity can be explained in part by the slow rates of convergence between the North American and Caribbean plates, calculated as 18–20 ± 3 mm yr^{-1} by DeMets *et al*. (2000), and more recently by DeMets *et al*. (2010) as 20 mm yr^{-1}. However, even at these low rates, the plate boundary accumulates enough strain per kilometre of arc each year for an earthquake of M_w 5.4, assuming a shear modulus of 45 GPa (using PREM below a depth of 15 km; Dziewonski & Anderson 1981), a downdip width of the seismogenic zone of 120 km (see Supporting Information), and 100 per cent coupling of the thrust interface. Over 300 km of arc (the rupture length of the 1843 event given by Feuillet *et al*. 2011), this equates to an M_w 7.0 earthquake every year—a clear indication that a significant amount of strain accumulated by plate motions along the Lesser Antilles Arc over the past 100+ yr has either been released aseismically, or has not been released to date, posing a significant hazard to the highly populated Caribbean region.

SEISMICITY ANALYSIS

We quantify the seismic hazard of this subduction zone in a similar manner to Hayes & Furlong (2010), by comparing strain accumulated via plate motions to seismic strain release along the arc (hereafter called moment deficit) calculated via the following steps:

(1) Using a combined EHB (Engdahl *et al*. 1998; Engdahl & Villaseñor 2002), PDE (USGS) and global centroid moment tensor (gCMT, http://www.globalcmt.org; Ekström *et al*. 2012) catalogue (using EHB where available and PDE otherwise to assure catalogue completeness for hypocentre locations; gCMT to provide mechanism information), we analyse earthquakes in the section of the Lesser Antilles subduction zone where convergence is occurring in a direction approximately perpendicular to the trench (i.e. we do not consider the Puerto Rico trench and areas farther west). We calculate the seismic moment, and approximate rupture length of each subduction-related earthquake in this region using the empirical relations of Blaser *et al*. (2010). We define an earthquake as subduction-related if it has a thrust-faulting mechanism whose slip vector aligns approximately with the plate motion direction, and whose hypocentral depth locates close to the subduction thrust interface (within depth uncertainties), computed using the method of Hayes *et al*. (2009) (see Supporting Information for slab geometry). If no mechanism is available (i.e. the earthquake is small), the event is considered subduction related if its depth locates close to the computed subduction interface. These small earthquakes do not significantly affect calculations because of their size, but their inclusion helps to assure completeness.

(2) Next, we divide the seismic moment of each event into moment per kilometre of rupture length, assuming each event nucleates in the centre of its ruptured fault.

(3) For each kilometre of arc in a direction parallel to the convergent plate boundary, we sum the total moment. An event contributes to the total moment in a particular location if its rupture length overlaps the location.

These calculations result in a measure of strain release over the time period of the catalogue (1973–present). We can extend these calculations back to 1900 using the Centennial Catalogue of Engdahl & Villaseñor (2002) and the new ISC-GEM catalogue (Storchak *et al*. 2013), incorporating an additional 17 Caribbean earthquakes of $M \geq 5.5$ that locate close to the subduction thrust interface. To account for moment 'missing' from this incomplete catalogue resulting from smaller earthquakes, we increase the total moment from earthquakes between 1900 and 1973 by 20 per cent (e.g. Bilham & Ambraseys 2005). This figure is compatible with modern magnitude-frequency relationships for the Lesser Antilles Arc, assuming the catalogue is complete at the *M*6.0–6.5 level.

We compare these calculations to expected total moment by calculating the potential moment (i.e. strain accumulation) per kilometre using:

$$m_0 = \mu A d, \quad (1)$$

where μ is the shear modulus ∼45 GPa (PREM; Dziewonski & Anderson 1981), A is the fault area = downdip seismogenic zone width and d is the slip = (plate rate × time period of catalogue).

For the Lesser Antilles subduction zone, we assume the downdip width of the seismogenic zone is ∼120 km (see Supporting Information for further discussion of downdip width and slab geometry), with a dip of 14° (Hayes *et al*. 2009), thus A ∼120 km^2; and NAM:CAR plate motion is ∼20 mm yr^{-1} (DeMets *et al*. 2000).

The results of this comparison along the Lesser Antilles subduction zone are shown in Fig. 3. Total moment of subduction-related earthquakes occurring along the arc is displayed as a percentage of plate motion accumulated over the length of the earthquake catalogue used—that is, 1900–present. This figure shows that, in most locations along the arc, less than 15 per cent of accumulated plate motion over the last 108 yr has been released seismically, leaving 80 per cent or more unaccounted for. These results are similar to those of Kagan (2002), who found seismic moment rates (sum of seismic moment of earthquakes/time span of catalogue) of 0.34–0.62 × 10^{18} N m yr^{-1}, and tectonic moment rates of 3.1–8.3 × 10^{18} N m yr^{-1}, implying ∼90 per cent of accumulated plate motion is unaccounted for seismically.

To assess how much of this moment deficit we can expect to be released seismically in future earthquakes (stored strain), we can turn to GPS studies which compare velocity of the upper plate as recorded at various points close to the plate boundary to plate motions, thus establishing where the interface is locked and where it is creeping. In the Caribbean, modelling by Manaker *et al*. (2008) estimated plate coupling ratios in the northern Lesser Antilles subduction zone at between 20 and 60 per cent (with uncertainties up to ±30 per cent), highest directly offshore of Guadeloupe. The difference between these coupling ratios and the percentage of moment released seismically over the past 108 yr provides an estimate of how much seismic potential energy is stored in the locked part of the subduction thrust. For example, our calculations imply that an earthquake bounded in the north by the Barracuda Ridge and in the south by either the Tiburon Ridge or the Saint Lucia Ridge (i.e. ∼200–350 km, of similar dimensions to estimates of the 1843 megathrust earthquake) could be as large as M_w 8.2 ± 0.2 (favoured scenario; Fig. 3; uncertainties discussed below). If these topographic highs do not act as barriers to rupture in a large earthquake, and instead the whole area analysed in this study ruptures in one event (∼650 km), there may be enough strain currently stored in the seismogenic zone to cause an earthquake of M_w 8.4 ± 0.2 (max. scenario).

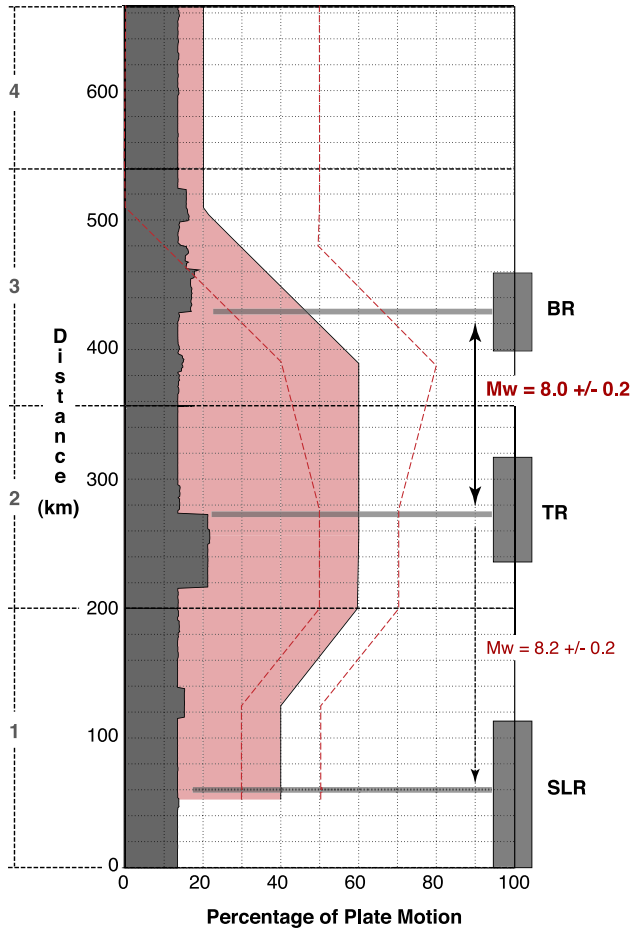

Figure 3. Results of our moment deficit calculations over the Lesser Antilles Trench study area. Shaded grey polygon represents the total moment of subduction-related earthquakes since 1900, per km of arc length, plotted as a percentage of plate motion accumulated over the same period. Shaded red polygon represents potential strain accumulated over this time period, from GPS-estimated coupling ratios (Manaker *et al*. 2008). Red dashed lines represent approximate uncertainties on those ratio estimates. Grey rectangles and bars represent the approximate projected locations of the Barracuda (BR), Tiburon (TR), and Saint Lucia (LCR) Ridges. These ridges act as potential barriers during earthquake rupture; should they act as barriers in a future earthquake, estimates of event maximum magnitude are shown adjacent to arrows representing the potential rupture length for two scenario earthquakes. The black solid arrow represents the minimum magnitude estimate for this rupture area; dashed represents the potential size if such an event were to extend beyond the Tiburon Ridge.

UNCERTAINTY

Accurately assessing how large a future earthquake can be in a given subduction zone is inherently difficult due to a number of complex uncertainties. For example, the role of so-called 'segment boundaries'—whether they be aseismic ridges, triple junctions, or some other bathymetric feature on the subducting plate—is not fully understood. In some cases, they seem to arrest rupture propagation (e.g. Collot *et al*. 2004), in others they do not (e.g. Taylor *et al*. 2008;

Furlong *et al*. 2009). These issues dictate the uncertainties on rupture length that we have introduced into our calculations, which vary here from 200 to 650 km. Furthermore, the up- and downdip limits of the seismogenic zone are not accurately known, and even though they may be estimated from the distribution of historic seismicity in a given subduction zone (e.g. Hayes *et al*. 2012; see Supporting Information), it is not clear whether very large earthquakes honour these bounds or rupture beyond them, particularly into the updip aseismic area of the subduction thrust (e.g. Hyndman 2007; Lay & Bilek 2007). The depth distribution of slip during the 1843 earthquake is also unclear, with some authors suggesting a rupture along the deeper portion of the interface (e.g. Feuillet *et al*. 2011). Because of these uncertainties, we have introduced a range of rupture widths into our calculations, varying from ∼80 to 140 km.

Shear modulus, or rigidity, is also not precisely known. We have assumed a global average appropriate for oceanic subduction zones in the depth range of interest (45 GPa); other studies of the Caribbean have used lower values of 35 GPa (Feuillet *et al*. 2011) and 30 GPa (ten Brink *et al*. 2011). For the purposes of assessing uncertainty, we have used a range of 30–45 GPa.

Additional uncertainties arise in relation to assessments of coupling ratios for the seismogenic zone. With the application of detailed GPS measurements above subduction zones, coupling ratios have become quantifiable, but uncertainties remain where data points are sparse and/or land area above the locked part of the subduction zone is limited. For our study, we have used coupling estimates from Manaker *et al*. (2008). Because station coverage in the central Lesser Antilles near Guadeloupe is fairly sparse, and observations are not ideally positioned with respect to the locked seismogenic zone, uncertainties from this study are fairly broad; approximately ±20–30 per cent. Uncertainty due to poorly constrained plate velocities and coupling ratios should decrease over time as long term, spatially dense GPS measurements become available through programs such as the 100-station COCONet (http://bit.ly/kRsrLP; Witze 2013). Until then, the Manaker *et al*. study provides the best-available model of coupling.

Incorporating these uncertainties into our calculations of moment deficit along the seismogenic zone of the Lesser Antilles arc leads to scenarios listed in Table S1. This shows that, depending on the combination of parameters and uncertainties, realistic potential earthquake magnitudes for this subduction zone range from M_w 7.6–8.6 (mostly dependent on how long a section ruptures at once). Using our favoured rigidity and coupling estimates ($\mu = 45$ GPa, coupling ∼40 per cent), enough stored strain exists for an earthquake of M_w 8.2 ± 0.2 (favoured scenario). These trade-offs are summarized graphically in Fig. 4, which reflects the trade-off between seismic coupling and earthquake size and their combined effect on the recurrence time of large earthquakes in the region. Given a rupture of the subduction zone offshore Guadeloupe between the Barracuda and Tiburon Ridges (M_w ∼ 8.0–8.2), and coupling estimates from Manaker *et al*. (20–60 per cent), the expected mean recurrence interval is between 80 and 400 yr. Since the 1843 earthquake was the largest historical event in the region (Shepherd 1992), which has been inhabited since at least the mid-17th century, the mean recurrence interval is likely to be at least the 170 yr that have passed since that event.

This analysis thus allows us to quantify a range of viable earthquake scenarios, and to show that regardless of the combination of parameters used the subduction zone to the east of the Lesser Antilles, particularly in the region offshore Guadeloupe, has stored enough energy over the past ∼110 yr to produce a large and potentially very damaging earthquake of magnitude M_w ∼ 8.2 ± 0.4

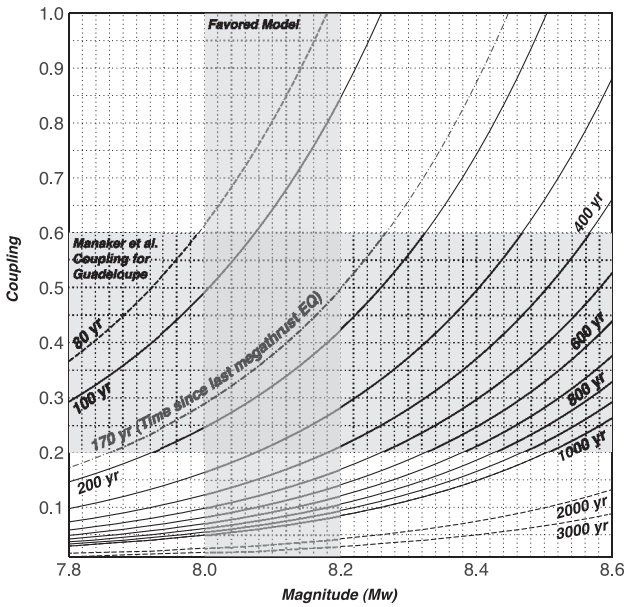

Figure 4. Inferred recurrence time of the Lesser Antilles megathrust adjacent to Guadeloupe as a function of earthquake magnitude and interface coupling, assuming that one major earthquake will account for most of the slip deficit calculated in this study. The grey shaded regions represent the coupling interpreted by Manaker *et al*. (2008) (horizontal) and the magnitude of our favoured earthquake scenario (vertical). Recurrence times are contoured (black lines). The time since the assumed last megathrust rupture (1843) is marked with a grey dot–dashed contour.

(spanning all scenarios). This is consistent with the corner magnitude for this region estimated by Kagan (2002) of M_c ∼ 8.76 ± 0.65. We infer that their value is higher because of their assumptions of seismogenic zone thickness (30 km—i.e. a seismogenic width of about 125 km), shear modulus (30 GPa), and most importantly a much higher seismic coupling of 100 per cent.

EARTHQUAKE AND TSUNAMI HAZARD POTENTIAL

Despite inherent uncertainty, it is clear from this study and from previous work that the Lesser Antilles subduction zone is capable of producing large and damaging earthquakes. This is of particularly concern given the vulnerability of communities and infrastructure in the Caribbean region as a whole, which has experienced significant population increase in the past 50 yr (Hyman 2005) and receives over 35 million visitors every year (Proenza & Maul 2010). The growth of large coastal cities and shipping harbours in this seismically active region often includes the construction of potentially unsafe buildings and infrastructure due to an insufficient knowledge of seismic hazard combined with limiting economic constraints. Minimization of the loss of life, infrastructure damage and economic impact due to earthquakes depends on accurate and reliable estimates of seismic hazard in the region.

Earthquake shaking

Given the combined vulnerability and hazard in the region, we attempt to quantify the risk posed by the scenario earthquakes outlined above using the USGS ShakeMap and PAGER software packages. ShakeMap (e.g. Wald *et al*. 2005) is a tool for representing the ground shaking produced by an earthquake, either via direct

Table 1. ShakeMap and PAGER scenarios, showing peak shaking intensities (Max MMI) and fatality and economic loss probability distributions for each of the 12 scenario earthquakes, computed for three different ground motion prediction equations. Model results are colour-coded by the likely overall alert level for each scenario; green representing no response necessary; yellow, regional response; orange, national response and red, international response. For each scenario, the most likely impact level is outlined in thick black pen. Keys for quantifying fatalities (number of people) and economic loss (millions of U.S. dollars) are displayed at the base of the table.

		Youngs97_interface			Zhao06_interface			Kanno2006		
		Max MMI	Fatalities	Economic Loss	Max MMI	Fatalities	Economic Loss	Max MMI	Fatalities	Economic Loss
Model 1	M7.8	VII	20% 33% 31% 13% 2%	5% 18% 34% 30% 12% 2%	VII+	18% 32% 32% 15% 3%	4% 16% 33% 31% 14% 3%	IX	4% 16% 33% 31% 13% 3%	1% 7% 24% 35% 24% 8%
	M8.0	VII	19% 33% 32% 14% 3%	4% 17% 33% 31% 13% 2%	VII+	15% 31% 33% 17% 4%	3% 14% 32% 32% 15% 3%	IX	2% 12% 29% 34% 18% 4%	3% 15% 33% 32% 17%
	M8.2	VII+	17% 32% 33% 15% 3%	4% 16% 33% 31% 14% 3%	VIII	13% 29% 34% 19% 5% 1%	2% 11% 29% 34% 19% 5% 1%	IX+	1% 9% 26% 35% 21% 6% 1%	2% 12% 30% 34% 22%
Model 2	M7.8	VII	22% 34% 30% 12% 2%	5% 18% 34% 29% 11% 2%	VII+	19% 33% 32% 14% 3%	4% 16% 33% 31% 13% 3%	VIII+	11% 27% 35% 21% 6% 1%	1% 5% 19% 35% 28% 10% 2%
	M8.0	VII	19% 33% 32% 14% 3%	4% 17% 34% 30% 12% 2%	VII+	16% 31% 33% 16% 3%	3% 15% 32% 32% 15% 3%	VIII+	6% 20% 35% 27% 10% 2%	2% 11% 28% 35% 19% 5%
	M8.2	VII+	18% 32% 32% 15% 3%	4% 16% 33% 31% 13% 3%	VIII	15% 31% 33% 17% 4%	3% 14% 32% 33% 15% 3%	VIII++	5% 18% 34% 30% 12% 2%	1% 9% 26% 35% 22% 7%
Model 3	M8.0	VII	19% 33% 32% 14% 3%	4% 17% 34% 30% 12% 2%	VII+	16% 31% 33% 16% 3%	3% 15% 32% 32% 14% 3%	VIII+	6% 20% 35% 28% 10% 2%	2% 11% 29% 35% 19% 5%
	M8.2	VII+	17% 32% 33% 15% 3%	4% 16% 33% 31% 13% 2%	VIII	15% 30% 34% 17% 4%	3% 14% 32% 32% 15% 3%	VIII++	4% 17% 34% 30% 12% 2%	1% 9% 26% 35% 22% 7%
	M8.4	VII+	16% 31% 33% 16% 3%	4% 15% 33% 31% 14% 3%	VIII+	12% 28% 35% 20% 5% 1%	1% 8% 25% 35% 22% 6% 1%	IX	4% 15% 33% 32% 14% 3%	1% 7% 24% 35% 24% 8%
Model 4	M8.0	VII+	18% 32% 32% 15% 3%	4% 17% 34% 30% 13% 2%	VIII	13% 29% 34% 18% 4%	3% 13% 31% 33% 16% 4%	IX	2% 10% 28% 35% 20% 5% 1%	3% 14% 32% 33% 19%
	M8.2	VII+	15% 31% 33% 17% 4%	3% 15% 32% 32% 15% 3%	VIII+	10% 26% 35% 22% 6% 1%	1% 7% 23% 35% 24% 8% 1%	IX+	1% 8% 25% 35% 23% 7% 1%	2% 11% 29% 34% 23%
	M8.4	VII+	13% 29% 34% 18% 4%	3% 13% 31% 33% 16% 3%	VIII+	8% 23% 35% 25% 8% 1%	4% 16% 33% 31% 13% 3%	X	1% 6% 22% 35% 26% 8% 1%	1% 9% 26% 35% 28%

Estimated Fatalities (number of people):

1 10 100 1,000 10,000 100,000

Estimated Economic Loss (USD millions):

1 10 100 1,000 10,000 100,000

Table 2. Tsunami heights (m) for each of 12 different earthquake scenarios, at 15 open ocean points shown in Fig. 5. The model highlighted in red is that shown in Fig. 5. Model parameters are listed in Table S1.

		1	2	3	4	5	6	7	8	9	10	11	12	13	14	15
Model 1	M7.8	0.11	0.18	0.24	0.32	0.14	0.15	0.12	0.13	0.48	0.17	0.37	0.66	0.23	0.17	0.14
	M8.0	0.23	0.31	0.51	0.63	0.31	0.32	0.27	0.27	0.98	0.31	0.85	1.41	0.51	0.36	0.28
	M8.2	0.42	0.52	0.87	1.15	0.59	0.60	0.50	0.51	1.79	0.50	1.50	2.48	0.96	0.65	0.52
Model 2	M7.8	0.17	0.21	0.44	0.36	0.21	0.22	0.22	0.30	0.54	0.27	0.44	0.59	0.34	0.25	0.23
	M8.0	0.34	0.38	0.87	0.70	0.40	0.44	0.43	0.60	0.97	0.44	0.83	1.10	0.67	0.44	0.46
	M8.2	0.64	0.77	1.69	1.36	0.78	0.86	0.83	1.17	1.65	0.71	1.60	2.20	1.30	0.85	0.90
Model 3	M8.0	0.30	0.37	0.65	0.53	0.29	0.27	0.27	0.38	0.45	0.31	0.50	0.57	0.39	0.29	0.28
	M8.2	0.59	0.74	1.28	1.04	0.57	0.54	0.54	0.76	0.89	0.50	0.99	1.17	0.77	0.56	0.56
	M8.4	1.18	1.52	2.53	1.92	1.13	1.07	1.08	1.48	1.70	0.85	1.99	2.38	1.52	1.06	1.09
Model 4	M8.0	0.23	0.30	0.58	0.33	0.25	0.26	0.27	0.35	0.43	0.31	0.49	0.49	0.30	0.31	0.24
	M8.2	0.46	0.60	1.02	0.64	0.49	0.50	0.53	0.70	0.81	0.52	0.93	0.94	0.59	0.57	0.47
	M8.4	0.92	1.20	2.03	1.34	0.97	1.01	1.05	1.39	1.42	0.83	1.83	1.82	1.19	1.01	0.94

observations from seismic data, or as predicted via ground motion prediction equations (GMPEs). It is used by the USGS for rapid earthquake response (Hayes *et al*. 2011) and, more recently, for quantifying the ground shaking effects of potential future earthquake scenarios. PAGER (prompt assessment of global earthquakes for response) is an automated system that provides estimates of the impacts of significant earthquakes around the world, and of the scope of the potential disaster, by correlating ShakeMaps with databases of population density and infrastructure vulnerability (Wald *et al*. 2008). Here we produce scenario ShakeMaps and PAGER reports (see Supporting Information) for earthquakes ranging from M_w 7.8 to 8.4, and varying in fault width (∼100–140 km) and length (∼200–350 km).

Due to the limited observations of strong ground shaking in the Lesser Antilles, we rely on previous studies of probabilistic seismic hazard in order to determine the most appropriate GMPEs to use for our analysis (Douglas & Mohais 2009; Bozzoni *et al*. 2011). These previous studies assessed several global GMPEs in order to determine which best represents the range of expected shaking intensities from Caribbean earthquakes. For larger magnitude crustal and subduction zone earthquakes, Japanese subduction zone GMPEs (Kanno *et al.* 2006, hereafter K06; Zhao *et al*. 2006, hereafter Z06) provide the best fit to the limited available instrumental data in the Lesser Antilles (Douglas & Mohais 2009). The GMPE of Youngs *et al*. (1997)—hereafter Y97—also fits reasonably well for both intraslab and interface earthquakes (Douglas & Mohais 2009) and provides our analysis with a conservative estimate of potential shaking (Bozzoni *et al*. 2011). These three models are compared in Fig. S6.

Results (Table 1; Fig. 5) show shaking from these scenario events will likely exceed MMI VII on Guadeloupe (even assuming the conservative Y97 GMPE) and could be as high as MMI IX–X (assuming K06). PAGER estimates suggest that fatalities for such events could range from below 100 (using Y97 or Z06) to as high ∼1000 (K06). Economic losses for such events may be as high as 100 billion U.S. dollars (K06), though are more likely in the range of 100 million to 1 billion U.S. dollars using more conservative GMPEs (Y97, Z06). These results show that, given the range of possible earthquake scenarios deemed plausible from our analyses, a significant national and potentially international disaster would occur as a result of earthquake shaking effects alone.

Tsunami hazard

In order to better understand tsunami hazards associated with the earthquake scenarios discussed above, we apply the numerical modelling used by Roger *et al*. (2013) to compute tsunami propagation. Tsunami wave height and inundation calculations are based on a numerical dispersion scheme and on solving the non-linear shallow-water equations in spherical coordinates. The initial deformation necessary to generate the tsunami is computed through an analytical numerical model of a rectangular fault plane rupture in an elastic half-space (Okada 1985). The seafloor deformation is transmitted to the sea surface without loss to an incompressible fluid (the ocean). Tsunami modelling was performed using code developed by the Commissariat à l'Energie Atomique, France (CEA; Heinrich *et al*. 1996), which solves the shallow water long wave hydrodynamic equations of continuity (2) and motion conservation (3):

$$\frac{\partial(\eta+h)}{\partial t}+\nabla\,.\,[v(\eta+h)]=0 \tag{2}$$

$$\frac{\partial v}{\partial t}+(v\,.\,\nabla)\,.\,v=-g\nabla\eta, \tag{3}$$

where η corresponds to water elevation, h to water depth, v to the horizontal speed vector and g to the gravity constant. Non-linear terms are taken into account, and the resolution is carried out using a Crank–Nicolson finite difference method centred in time and using an upwind scheme in space. Bottom friction is not included in this calculation, which may cause wave coastal amplification factors (i.e. shallow water wave speed and height) to be slightly overestimated, but which has little effect on deep-water results. Wave propagation is calculated using a two-way grid-nesting scheme over three levels of nested grids from Roger *et al*. (2013). Bathymetric grids are prepared using multibeam data from the Hydrographic and Oceanographic Service of the French Navy (SHOM), combined with georeferenced and digitized nautical charts of Guadeloupe Archipelago (SHOM, 1994, 2008), the ETOPO 1 Global Relief Model data set (Amante & Eakins 2009) and SRTM 3″ (Farr *et al*. 2007). Kriging interpolation of this data set has been applied to produce the regular grids necessary to input in the modelling code. The first grid (Grid 0) has a spatial resolution of 1′ and represents the Northern part of the Lesser Antilles Arc. Grid 2 is a 500 m resolution grid extending from Antigua (in the north) to Guadeloupe and Dominica (in the south). Grid 3 includes the Guadeloupe Archipelago at a resolution of ∼150 m. Tsunami calculation results are represented by maximum wave height maps corresponding to the maximum sea level reached during the propagation (1h30) at each gridpoint. This method has been widely used in the literature for similar analyses (e.g. Hébert *et al*. 2001; Roger & Hébert 2008; Allgeyer *et al*. 2012).

Tsunami wave heights calculated for the range of scenario earthquakes are displayed in Table 2 for 15 points in deep water around the Guadeloupe Archipelago (tsunami modelling parameters given in Table S2). Fig. 5 shows the location of these points, and the maximum wave height for model 2 assuming an M_w 8.0 earthquake. Note that tsunami heights between these 15 points and the respective shores increase—significantly, in some cases—since shallow bathymetry and shoaling effects amplify wave heights approaching coastlines. The tsunami modelling results demonstrate that even for earthquakes at the lower end of our magnitude range, wave heights at local Caribbean Islands would be on the meter scale—over 3 m in several locations. Our results are consistent with Roger *et al*. (2013), who also show that specific coastal 'hotspots' can considerably amplify the tsunami wave arrival due to local bathymetry, wave shoaling and resonance phenomena (Fig. 5). It is significant to note that many of these coastal areas coincide with communities with the highest local and tourist populations; large tsunami heights are modelled for the Guadeloupe population centres of Grande Anse (Fig. 5 point 12, population ∼2000); Sainte-Francois (point 11, population ∼13 000); Sainte-Anne (point 9, population ∼23 000); Le Gosier (point 7, population ∼29 000); Pointe-a-Pitre (point 10, population ∼18 000) and Petit-Bourg (point 8, population ∼25 000). Arrival times of our modelled tsunamis on the shores of Guadeloupe range from 10 to 30 min from east to west across the island.

The 'short fuse' local tsunami scenario described in this study would provide very little preparation time for the island communities of Guadeloupe. As witnessed in the Japan tsunami of 2011 March, even well-prepared communities with adequate warning systems are not necessarily able to react in time to minimize extensive loss of life and infrastructure damage.

CONCLUSIONS

In this study, we quantify the seismic and tsunami hazard in the Lesser Antilles subduction zone, focusing on the plate interface

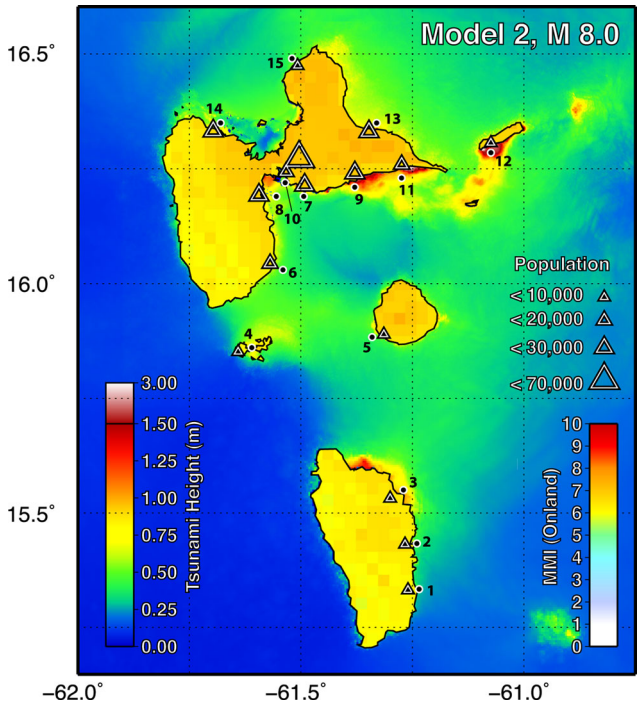

Figure 5. Earthquake shaking (onland) and tsunami (ocean) hazard in Guadeloupe and Dominica, as a result of an *M*8.0 earthquake on the Lesser Antilles megathrust adjacent to Guadeloupe (see Table S1 for earthquake model parameters). Colours onland represent scenario earthquake shaking intensities calculated in USGS ShakeMap software (Wald *et al*. 2005). Colours in the ocean represent modelled tsunami heights from the same earthquake scenario. Major population centres are plotted with triangles, sized according to their populations. Numbered circles are points where open ocean tsunami heights have been calculated for each earthquake scenario and are listed in Table 2.

offshore of Guadeloupe. Our results suggest that enough strain is currently stored in this seismogenic zone to cause a large and damaging earthquake of magnitude $M_w \sim 8.2 \pm 0.4$ (spanning all scenarios). Such an earthquake is capable of significant damage due to high levels of ground shaking (MMI VIII-X), and would generate a tsunami with maximum wave heights on the order of 3 m in the Guadeloupe Archipelago.

We provide here PAGER loss estimates for scenario earthquakes (Table 2; Supporting Information) to help mitigate possible loss of life and economic impact resulting from future earthquakes. U.S. (USGS, NOAA) and international (UNESCO) efforts to improve earthquake (McNamara *et al*. 2006) and tsunami monitoring (McNamara *et al*. 2009) in the Caribbean region should contribute to necessary tsunami disaster mitigation.

While significant progress has been made to improve earthquake and tsunami monitoring in the Caribbean region, warning capabilities are not yet at the same standard as exists in the northern Pacific. Recommendations for improved tsunami disaster mitigation and warning include: increases in real-time transmission of seismic and sea level data; robust communication systems for the dissemination and reception of warnings; improved tsunami inundation models; detailed near-coastal bathymetry; preparedness, education and outreach to create tsunami-resilient communities; and focusing of international tsunami warning systems on the ocean basins of the Caribbean and Atlantic. With programs such as CO-CONet (http://bit.ly/kRsrLP; Witze 2013), some of these necessary improvements are underway.

ACKNOWLEDGEMENTS

Figures in this manuscript were made using the Generic Mapping Tools software package (Wessel & Smith 1991). Gebco2008 bathymetry is used for all basemaps. We thank Uri ten Brink, Eric Geist, Christa von Hillebrandt, and two anonymous reviewers for reviews and constructive comments that have helped improve this manuscript. Any use of trade, product, or firm names is for descriptive purposes only and does not imply endorsement by the U.S. Government.

REFERENCES

Allgeyer, S., Daubord, C., Hébert, H., Loevenbruck, A., Schindelé, F. & Madariaga, R., 2012. Could a 1755-Like tsunami reach the French Atlantic coastline? Constraints from twentieth century observations and numerical modeling, *Pure appl. Geophys.,* **170,** 1415–1431.

Amante, C. & Eakins, B.W., 2009. ETOPO1 1 arc-minute global relief model: procedures, data sources and analysis, NOAA Technical Memorandum NESDIS, NGDC-24, 19 pp.

Bernard, P. & Lambert, J., 1988. Subduction and seismic hazard in the northern Lesser Antilles: revision of the historical seismicity, *Bull. seism. Soc. Am.,* **78,** 1965–1983.

Bilham, R. & Ambraseys, N., 2005. Apparent Himalayan slip deficit from the summation of seismic moments for Himalayan earthquakes, 1500–2000, *Curr. Sci.,* **88,** 1658–1663.

Blaser, L., Kruüger, F., Ohrnberger, M. & Scherbaum, F., 2010. Scaling relations of earthquake source parameter estimates with special focus on subduction environment, *Bull. seism. Soc. Am.,* **100,** 2914–2926.

Bouysse, P. & Westercamp, D., 1990. Subduction of Atlantic aseismic ridges and late Cenozoic evolution of the Lesser Antilles island arc, *Tectonophysics,* **175,** 349–380.

Bozzoni, F. *et al.*, 2011. Probabilistic seismic hazard assessment at the eastern Caribbean Islands, *Bull. seism. Soc. Am.,* **101,** 2499–2521.

ten Brink, U.S. & Lin, J., 2004. Stress interaction between subduction earthquakes and forearc strike-slip faults: Modeling and application to the northern Caribbean plate boundary, *J. geophys. Res.,* **109,** B12310, doi:10.1029/2004JB003031.

ten Brink, U.S., Bakun, W.H. & Flores, C.H., 2011. Historic perspective on seismic hazard to Hispaniola and the northeast Caribbean region, *J. geophys. Res.,* **116,** B12318, doi:10.1029/2011JB008497.

ten Brink, U.S., Marshak, S. & Granja-Bruna, J.L., 2009. Bivergent thrust wedges surrounding oceanic island arcs: Insight from observations and sandbox models of the northeastern Caribbean plate, *Geol. Soc. Am. Bull.,* **121,** 1522–1536.

Calais, E., Perrot, J. & Mercier de Lépinay, B., 1998. Strike-slip tectonics and seismicity along the northern Caribbean plate boundary from Cuba to Hispaniola, *Geol. Soc. Am. Special Paper,* **326,** 125–142.

Collot, J-Y. *et al.*, 2004. Are rupture zone limits of great subduction earthquakes controlled by upper plate structures? Evidence from multichannel seismic reflection data acquired across the northern Ecuador–southwest Colombia margin, *J. geophys. Res.,* **109,** doi:10.1029/2004JB003060.

DeMets, C., Gordon, R.G. & Argus, D.F., 2010. Geologically current plate motions, *Geophys. J. Int.,* **181,** 1–80.

DeMets, C., Jansma, P.E., Mattioli, G.S., Dixon, T.H., Farina, F., Bilham, R., Calais, E. & Mann, P., 2000. GPS geodetic constraints on Caribbean-North America plate motion, *Geophys. Res. Lett.,* **27,** 437–440.

Dolan, J.F. & Wald, D.J., 1998. The 1943–1953 north-central Caribbean earthquakes: active tectonic setting, seismic hazards, and implications for Caribbean–North America plate motions, *Geol. Soc. Am. Special Paper,* **326,** 143–170.

Douglas, J. & Mohais, R., 2009. Comparing predicted and observed ground motions from subduction earthquakes in the Lesser Antilles, *J. Seismol.,* **13,** 577–587.

Dziewonski, A.M. & Anderson, D.L., 1981. Preliminary reference Earth model, *Phys. Earth planet. Inter.,* **25,** 297–356.

Ekström, G., Nettles, M. & Dziewoński, A.M., 2012. The global CMT project 2004–2010: centroid-moment tensors for 13,017 earthquakes, *Phys. Earth planet. Inter.,* **200–201,** 1–9.

Engdahl, E.R. & Villaseñor, A., 2002. Global Seismicity: 1900–1999, in *International Handbook of Earthquake and Engineering Seismology, Part A,* Chapter 41, pp. 665–690, eds Lee, W.H.K., Kanamori, H., Jennings, P.C. & Kisslinger, C., Academic Press.

Engdahl, E.R., Van Der Hilst, R.D. & Buland, R.P., 1998. Global teleseismic earthquake relocation with improved travel times and procedures for depth determination, *Bull. seism. Soc. Am.,* **88,** 722–743.

Farr, T.G. *et al.*, 2007. The shuttle radar topography mission. *Rev. Geophys.,* **45,** RG2004, doi:10.1029/2005RG000183.

Feuillet, N., Beauducel, F. & Tapponnier, P., 2011. Tectonic context of moderate to large historical earthquakes in the Lesser Antilles and mechanical coupling with volcanoes, *J. geophys. Res.,* **116,** B10308, doi:10.1029/2011JB008443.

Feuillet, N., Manighetti, I. & Tapponnier, P., 2002. Arc parallel extension and localization of volcanic complexes in Guadeloupe, Lesser Antilles, *J. geophys. Res.,* **107,** doi:10.1029/2001JB000308.

Furlong, K.P., Lay, T. & Ammon, C., 2009. A great earthquake rupture across a rapidly evolving three-plate boundary, *Science,* **324,** 226–229.

Geist, E.L. & Parsons, T., 2009. Assessment of source probabilities for potential tsunamis affecting the U.S. Atlantic Coast, *Mar. Geol.,* **264,** 98–108.

Geist, E.L., Parsons, T., ten Brink, U.S. & Lee, H.J., 2009. Tsunami probability, in *The Sea,* Vol 15, pp. 93–135, eds Bernard, E.N. & Robinson, A.R., Harvard University Press.

Hayes, G.P. & Furlong, K.P., 2010. Quantifying potential tsunami hazard in the Puysegur subduction zone, south of New Zealand, *Geophys. J. Int.,* **183**(3), 1512–1524.

Hayes, G.P., Wald, D.J. & Keranen, K., 2009. Advancing techniques to constrain the geometry of the seismic rupture plane on subduction interfaces *a priori*—higher order functional fits, *Geochem. Geophys. Geosyst.,* **10,** Q09006, doi:10.1029/2009GC002633.

Hayes, G.P., Earle, P.S., Benz, H.M., Wald, D.J. & Briggs, R.W. & the USGS/NEIC Earthquake Response Team, 2011. 88 Hours: the U.S. Geological Survey National Earthquake Information Center response to the 11 March 2011 Mw 9.0 Tohoku earthquake, *Seismol. Res. Lett.,* **82,** 481–493.

Hayes, G.P., Wald, D.J. & Johnson, R.L., 2012. Slab1.0: a three-dimensional model of global subduction zone geometries, *J. geophys. Res.,* **117,** B01302, doi:10.1029/2011JB008524.

Hébert, H., Heinrich, P., Schindelé, F. & Piatanesi, A., 2001. Far-field simulation of tsunami propagation in the Pacific Ocean: impact on the Marquesas Islands (French Polynesia), *J. geophys. Res.,* **106,** 9161–9177.

Heinrich, P., Guibourg, S. & Roche, R., 1996. Numerical modeling of the 1960 Chilean tsunami. Impact on French Polynesia, *Phys. Chem. Earth,* **21**(12), 19–25.

Hough, S.E., 2013. Missing great earthquakes, *J. geophys. Res.,* **118,** 1098–1108.

Hyman, G., 2005. Centro Internacional de Agricultura Tropical (CIAT), United Nations Environment Program (UNEP), Center for International Earth Science Information Network (CIESIN), Columbia University, and the World Bank Latin American and Caribbean Population Database, Version 3, Available at: http://www.na.unep.net/datasets/datalist.php3 or http://gisweb.ciat.cgiar.org/population/dataset.htm (last accessed 17 October 2013).

Hyndman, R.D., 2007. The seismogenic zone of subduction thrust faults: What we know and don't know, in *The Seismogenic Zone of Subduction Thrust Faults,* pp. 15–35, eds Dixon, T.H. & Moore, J.C., Columbia Univ. Press.

Jordan, T.H., 1975. The present-day motions of the Caribbean plate, *J. geophys. Res.,* **80,** 4433–4439.

Kagan, Y.Y., 2002. Seismic moment distribution revisited: II. Moment conservation principle, *Geophys. J. Int.,* **149,** 731–754.

Kanno, T., Narita, A., Morikawa, N., Fujiwara, H. & Fukushima, Y., 2006. A new attenuation relation for strong motion in Japan based on recorded data, *Bull. seism. Soc. Am.,* **96**(3), 879–897.

Laigle, M. *et al.*, 2013. Along-arc segmentation and interaction of subducting ridges with the Lesser Antilles subduction forearc crust revealed by MCS imaging, *Tectonophysics,* **603,** 32–54.

Lay, T. & Bilek, S., 2007. Anomalous earthquake ruptures at shallow depths on subduction zone megathrusts, in *The Seismogenic Zone of Subduction Thrust Faults,* pp. 476–511, eds Dixon, T.H. & Moore, J.C., Columbia Univ. Press.

Le Friant, A., Heinrich, P. & Boudon, G., 2008. Field survey and numerical simulation of the 21 November 2004 tsunami at Les Saintes (Lesser Antilles), *Geophys. Res. Lett.,* **35**(12), doi:10.1029/2008GL034051.

Lynch, L.L. & Shepherd, J.B., 1995. An earthquake catalogue for the Caribbean Part II, the macroseismic listing for the instrumental period 1900–1991, *Prepared for Presentation at the Meeting of the Caribbean and Latin American Seismic Hazard Project Workshop,* May, Melbourne, Florida.

McCann, W.R. & Sykes, L.R., 1984. Subduction of aseismic ridges beneath the Caribbean Plate: implications for the tectonics and seismic potential of the northeastern Caribbean, *J. geophys. Res.,* **89,** 4493–4519.

McNamara, D., McCarthy, J. & Benz, H., 2006. Improving Earthquake and Tsunami Warning for the Caribbean Sea, Gulf of Mexico and the Atlantic Coast, U.S. Geol. Surv. Fact Sheet, 2006–3012, 4 p, (http://pubs.usgs.gov/fs/2006/3012/).

McNamara, D.E., von Hillebrandt-Andrade, C., Earle, P. & Buland, R., 2009. Seismic capabilities of an international Caribbean tsunami warning system, *Seismol. Res. Lett.,* **80**(2), 344.

Manaker, D.M. *et al.*, 2008. Interseismic plate coupling and strain partitioning in the northeastern Caribbean, *Geophys. J. Int.,* **174,** 889–903.

Mann, P., Taylor, F.W., Edwards, R.L. & Ku, T.-L., 1995. Actively evolving microplate formation by oblique collision and sideways motion along strike-slip-faults: an example from the northeastern Caribbean plate margin, *Tectonophysics,* **246,** 1–69.

Mann, P., Calais, E., Ruegg, J.-C., DeMets, C., Jansma, P.E. & Mattioli, G.S., 2002. Oblique collision in the northeastern Caribbean from GPS measurements and geological observations, *Tectonics,* **21,** doi:10.1029/2001TC001304.

Mann, P., Hippolyte, J-C., Grindlay, N.R. & Abrams, L.J., 2005. Neotectonics of southern Puerto Rico and its offshore margin, *Geol. Soc. Am. Special Paper,* **385,** 173–214.

Okada, Y., 1985. Surface deformation due to shear and tensile faults in a half-space, *Bull. seism. Soc. Am.,* **75,** 1135–1154.

O'Loughlin, K.F. & Lander, J.F., 2003. *Caribbean Tsunamis: A 500-Year History from 1498–1998*, Kluwer.

Parsons, T. & Geist, E.L., 2008. Tsunami probability in the Caribbean region, *Pure appl. Geophys.,* **165,** 2089–2116.

Pelinovsky, E., Zahibo, N., Dunkley, P., Edmonds, M., Herd, R., Talipova, T., Kozelkov, A. & Nikolkina, I., 2004. Tsunami generated by the volcano eruption on July 12–13 2003 at Montserrat, Lesser Antilles, *Sci. Tsunami Hazards,* **22,** 44–57.

Prentice, C.S., Mann, P., Peña, L.R. & Burr, G., 2003. Slip rate and earthquake recurrence along the central Septentrional fault, North American–Caribbean plate boundary, Dominican Republic, *J. geophys. Res.* **108,** doi:10.1029/2001JB000442.

Proenza, X.W. & Maul, G.A., 2010. Tsunami hazard and total risk in the Caribbean basin, *Sci. Tsunami Hazards,* **29**(2), 70–77.

Robson, G.R., 1964. An earthquake catalogue for the Eastern Caribbean, *Bull. seism. Soc. Am.,* **54,** 785–832.

Roger, J. & Hébert, H., 2008. The Djijelli (Algeria) earthquake and tsunami: source parameters and implications for tsunami hazard in the Balearic Islands, *Nat. Hazards Earth Syst. Sci.,* **8,** 721–731.

Roger, J., Baptista, M.A., Sahal, A., Allgeyer, S. & Hébert, H., 2010a. The transoceanic 1755 Lisbon tsunami in Martinique, *Pure appl. Geophys.* [Proceedings of the International Tsunami Symposium, Novosibirsk, Russia, July 2009], **168**(6–7), 1015–1031.

Roger, J., Allgeyer, S., Hébert, H., Baptista, M.A., Loevenbruck, A. & Schindelé, F., 2010b. The 1755 Lisbon tsunami in Guadeloupe Archipelago: source sensitivity and investigation of resonance effects, *Open Oceanogr. J.,* **4,** 58–70.

Roger, J., Dudon, B. & Zahibo, N., 2013. Tsunami hazard assessment of Guadeloupe Island (F.W.I.) related to a megathrust rupture on the Lesser Antilles subduction interface, *Nat. Hazards Earth Syst. Sci.,* **13,** 1–15.

Shepherd, J.B., 1992. Comment on "Subduction and seismic hazard in the Lesser Antilles" by Pascal Bernard and Jerome Lambert, *Bull. seism. Soc. Am.,* **82,** 1534–1543.

Shepherd, J.B. & Lynch, L.L., 1992. An earthquake catalogue for the Caribbean Part I, the pre-instrumental period 1502–1900, *Paper Presented to the Meeting of the Steering Committee,* Latin American and Caribbean Seismic Hazard Programme, April, Melbourne, Florida.

Stein, S., Engeln, J.F., Weins, D.A., Fujita, K. & Speed, R.C., 1982. Subduction seismicity and tectonics in the Lesser Antilles arc, *J. geophys. Res.,* **87,** 8642–8664.

Storchak, D.A., Di Giacomo, D., Bondár, I., Engdahl, E.R., Harris, J., Lee, W.H.K., Villaseñor, A. & Bormann, P., 2013. Public release of the ISC-GEM Global Instrumental Earthquake Catalog (1990–2009), *Seismol. Res. Lett.,* **84**(5), 810–815.

Taylor, F.W., Briggs, R.W., Frohlich, C., Brown, A., Hornbach, M., Papabatu, A.K., Meltzner, A.J. & Billy, D., 2008. Rupture across arc segment and plate boundaries in the 1 April 2007 Solomons earthquake, *Nat. Geo.,* **1,** 253–257.

Wald, D.J., Worden, B.C., Lin, K. & Pankow, K., 2005. ShakeMap manual: technical manual, user's guide, and software guide, U.S. Geological Survey, Techniques and Methods, 12-A1, 132 pp.

Wald, D.J., Earle, P.S., Porter, K., Jaiswal, K. & Allen, T.I., 2008. Development of the U.S. Geological Survey's Prompt Assessment of Global Earthquakes for Response (PAGER) System, in *Proceedings of the 14th World Conf. on Earthq. Eng.,* Beijing, 10 p.

Weber, J.C. *et al.*, 2001. GPS estimate of relative motion between the Caribbean and South American plates, and geologic implications for Trinidad and Venezuela, *Geology,* **29,** 75–78.

Wessel, P. & Smith, W., 1991. Free software helps display data, *EOS, Trans. Am. geophys. Un.,* **72,** 445–446.

Witze, A., 2013. A network to track Caribbean hazards, *Nature,* **497,** 421–422.

Youngs, R.R., Chiou, S.-J., Silva, W.J. & Humphrey, J.R., 1997. Strong Ground Motion Attenuation Relationships for Subduction Zone Earthquakes, *Seismol. Res. Lett.,* **68,** 58–73.

Zahibo, N., Pelinovsky, E., Yalciner, A.C., Kurkin, A., Koselkov, A. & Zaitsev, A., 2003. The 1867 Virgin Island Tsunami, *Nat. Hazards Earth Syst. Sci.,* **3,** 367–376.

Zahibo, N., Pelinovsky, E., Yalciner, A., Zaitsev, A., Talipova, T., Nikolkina, I. & Chernov, A., 2011. Trans-Atlantic propagation of 1755 tsunami and its effects on the French West Indies, *Open Oceanogr. J.,* **5,** 30–41.

Zhao, J.X. *et al.*, 2006. Attenuation relations of strong ground motion in Japan using site classification based on predominant period, *Bull. seism. Soc. Am.,* **96,** 898–913.

SUPPORTING INFORMATION

Additional Supporting Information may be found in the online version of this article:

Figure S1. Seismicity basemap, showing earthquakes from a combined EHB and USGS PDE catalogue (light outlines), and the ISC-GEM catalogue (dark outlines), sized by magnitude and coloured by depth. Moment tensors are from the global CMT catalogue. Lines of white circles labelled 1–3 are the locations of cross-sections shown in Figs S2–S4. Grey circles mark the origin of those cross-sections.

Figure S2. Cross-section 1, beneath Guadeloupe (marked on *Y*-axis). Light grey circles with black outlines are from a combined EHB and USGS PDE catalogue; darker circles with red outlines from the ISC-GEM catalogue. Moment tensors, plotted in cross-section (rear-hemisphere) are from the global CMT catalogue. Red diamonds represent local active source seismic data (Hayes *et al*. 2012). The black curve represents the approximate geometry of the local subducting slab.

Figure S3. Cross-section 2, beneath Martinique. See Fig. S2 caption for details.

Figure S4. Cross-section 3, beneath Barbuda. See Fig. S2 caption for details.

Figure S5. Depth distribution of thrust (i.e. subduction related) seismicity in cross-sections 1–3 (Figs S1–S4). Data are fit with normal (red) and double-normal (black dashed) distributions, based on whether deeper seismicity (dark grey bars) with larger misfits between nodal plane dips and the slab interface are interpreted as inter- or intraplate events.

Figure S6. Comparisons between the ground motion prediction equations of Kanno *et al*. (2006; red), Youngs *et al*. (1997; blue) and Zhao *et al*. (2006; yellow), plotted as ground acceleration versus distance from the source.

Table S1. Earthquake scenario moment deficit calculations and uncertainties. Given estimates for rigidity ('mu', GPa), rupture length ('L', km), rupture width ('W', km), plate motion ('PM', m yr^{-1}) and geodetic coupling ('Coupling', per cent), we calculate accumulated moment deficit ('Acc. Mo.', N m) and associated potential magnitude (M_w). Models using favoured parameters are highlighted in red, and correspond to the scenarios shown in Fig. 3 and discussed in the main text.

Table S2. Seismogenic zone parameters used for tsunami models (corresponding to Table 2). Parameters for each model are the same as model above, unless otherwise stated (http://gji.oxfordjournals.org/lookup/suppl/doi:10.1093/gji/ggt385/-/DC1).

Please note: Oxford University Press is not responsible for the content or functionality of any supporting materials supplied by the authors. Any queries (other than missing material) should be directed to the corresponding author for the article.